Heliyon 12 (2026) e44424

Contents lists available at ScienceDirect

Heliyon

journal homepage: www.cell.com/heliyon

Research article

The harmonic-dominant signals in animal communication involve the use of new resonant frequencies

Teddy Gaiddon [a,*], Thorin Jonsson [b], Alberto Mittone [c], Alberto Bravin [d], Fernando Montealegre-Z [e], Vincent Tournat [f], Tony Robillard [a]

[a] Institut de Systématique, Evolution et Biodiversité (ISYEB), Muséum national d'Histoire naturelle, CNRS, SU, EPHE-PSL, UAA, 57 rue Cuvier, CP 50, Paris, 75231, France
[b] Institute of Biology, Karl-Franzens-University Graz, Graz, Austria
[c] Argonne National Laboratory Advanced Photon Source: Lemont, IL, USA
[d] Università degli Studi di Milano-Bicocca Dipartimento di Fisica Giuseppe Occhialini: Milano, Lombardia, Italy
[e] School of Natural Sciences, Joseph Banks Laboratories, University of Lincoln, Lincoln, United Kingdom
[f] Laboratoire d'Acoustique de l'Université du Mans (LAUM), UMR 6613, Institut d'Acoustique - Graduate School (IA-GS), CNRS, Le Mans Université, France

ARTICLE INFO

Keywords:
Bioacoustics
Stridulation
Finite element modelling
Harmonic-hopping
Eneopterinae

ABSTRACT

Acoustic signals in animals are classically produced using source-filter mechanisms. Many species are capable of producing high-frequency sounds characterised by dominant harmonic frequencies. These signals emerged following an evolutionary phenomenon known as "harmonic-hopping". The study of the source-filter mechanism of Eneopterinae crickets suggests that emergence of harmonic-dominant signals is linked to changes in the physical properties of the filter. To test this hypothesis, we used laser Doppler vibrometry and finite element modelling to characterise the vibro-acoustic behaviour of the sound-producing forewings of two species of Eneopterinae crickets. Our results suggest that the forewing venation plays a key constraining role distinguishing the two species' respective vibro-acoustic behaviours. Our results also highlight the role of the membrane deformation and the damping properties of the forewings in the sound-producing mechanism of these crickets. We suggest that harmonic-hopping may be associated with the emergence of new resonant frequencies in the forewings of Eneopterinae crickets.

1. Introduction

Animal communication signals are the vectors of interactions between individuals, either at the intraspecific level, by playing a major role in reproduction or sociality, or at the interspecific level, in the mechanisms involved in competition and predation [1]. Acoustic signals in the living world are classically produced by specialised structures via a common mechanism, modelled as the source-filter mechanism [2]. This model is divided into two distinct parts. The first, called the source, is made up of structures that enable the organism to produce periodic series of pulses of mechanical energy (e.g, the vibration of the vocal cords within the larynx in mammals), which are transmitted to the second part, the filter. The filter is made up of resonant structures (e.g., the vocal tract in mammals), whose resonance amplifies certain frequencies of the source signal. The sounds produced at the system's output are

* Corresponding author.
E-mail address: teddy.gaiddon1@mnhn.fr (T. Gaiddon).

https://doi.org/10.1016/j.heliyon.2025.e44424
Received 19 September 2024; Received in revised form 12 December 2025; Accepted 16 December 2025
Available online 8 January 2026

therefore the product of the interaction between the periodic signal from the source and the resonant properties of the filter. The source and filter are considered independent in the original description of the model, but variants where the two parts are coupled have subsequently been described [3]. The sounds produced by the source-filter mechanism are classically composed of a dominant fundamental frequency (the dominant frequency of the source signal, which carries most of the energy in the sound spectrum) and can be enriched with harmonic frequencies (integer multiples of this fundamental frequency) [4]. However, in the great diversity of acoustic signals produced by animals, many species emit sounds characterised by dominant harmonic frequencies, i.e. where the frequency carrying the most energy in the signal is no longer the fundamental, but one of the harmonic frequencies. Such harmonic-dominant signals are present in many different taxonomic groups, in mammals (manatees [5], cetaceans [6], bats [7]); hummingbirds [8]; anurans [9]; and orthopterans [10]. This causes the sounds produced by these species to have a higher frequency than the average frequency range of other species in the same group and may be correlated with selective advantages for the individuals producing these sounds [11]. While the ecological aspects and behavioural consequences of these specific signals are often studied, their physical and evolutionary origins have rarely been investigated.

In the last two decades, a small number of studies have dealt with the evolutionary history of harmonic-dominant signals produced by three different groups of animals: hummingbirds in the genus *Selasphorus* [3], horseshoe bats of the family Rhinolophidae [7], and crickets of the subfamily Eneopterinae [11]. These studies have revealed the presence of transitions of dominance between harmonically-related frequency peaks in the sound spectrum of these animals over the course of evolutionary history. Such transitions occurred either between the fundamental frequency and one of the harmonics, or between two different harmonic frequencies. This evolutionary phenomenon has been called “harmonic-hopping” [7], due to the change of the dominant frequency from an ancestral state to another, apparently without passing through intermediate frequencies.

Eneopterinae crickets are a tropical subfamily of Gryllidae (Insecta, Orthoptera) containing more than 290 species, the majority belonging to the tribe Lebinthini (ca. 180 species) [12]. Lebinthini crickets are known for their production of high-frequency acoustic signals [13]. As with the vast majority of species in the Gryllidae family, the males of Eneopterinae crickets emit calling songs to attract female's attention for reproduction. However, whereas the callings songs produced by the majority of crickets are characterised by a dominant frequency ranging between 2 and 8 kHz [14], species of the Lebinthini tribe produce high-frequency songs whose dominant frequencies range between 10 and 28 kHz [13]. Futhermore, the calling songs of many Eneopterinae crickets are characterised by the presence of high-amplitude harmonic frequencies [15]. In most species of the speciose Lebinthini tribe, the dominant frequency of the calling song spectrum is a harmonic frequency of the low-amplitude fundamental. Several studies revealed that the evolutionary origin of the high-frequency signals in this tribe is due to multiple harmonic-hopping events [11,13] over the course of evolutionary history (Fig. 1A).

Sound production in crickets is a well-understood two-step process [16]. Like other animals, crickets produce acoustic signals by means of a source-filter mechanism, using a set of structures on their forewings called "the stridulatory apparatus". The source of the

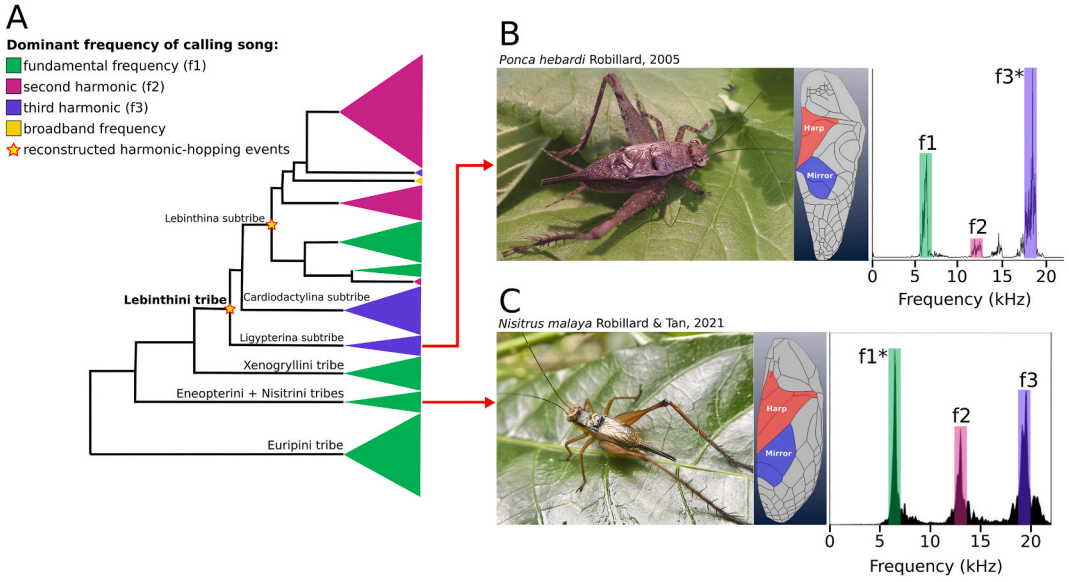

Fig. 1. Harmonic-hopping in the Eneopterinae subfamily. A Simplified phylogenetic tree of the Eneopterinae subfamily indicating the nature of the dominant frequency of the male's calling song, reconstructed harmonic-hopping events, and phylogenetic position of the two species of interest (inspired by Tan et al., 2021) [13]. B Photograph of a male of the species *Ponca hebardi*, accompanied by a representation of the dorsal field of the left forewing, showing the main resonant cells of the membrane known as the harp (in red) and the mirror (in blue), and image of the acoustic power spectrum of the male's calling song showing its harmonic structure. C Photograph of a male of the species *Nisitrus malaya*, accompanied by a representation of the dorsal field of the left forewing, showing the main resonant cells of the membrane known as the harp (in red) and the mirror (in blue), and image of the acoustic power spectrum of the male's calling song showing its harmonic structure. The dominant frequency of each species' acoustic power spectrum is indicated by an asterisk.

crickets' sound-producing mechanism consists of two distinct parts: the stridulatory file is a modified vein carrying a series of cuticular teeth located on the ventral side of the right forewing, and the plectrum, a thickened edge of the left forewing, which is located underneath the right forewing. The first step of sound production is called the stridulation process, in which the male moves his raised forewings in an opening-closing motion, causing the plectrum to rub against the teeth of the file in series each time the forewings close. It is this friction that produces a vibratory signal, corresponding to the source signal. The dominant frequency of the source signal depends directly on the number of teeth struck by the plectrum during a unit of time, a quantity called "tooth-strike rate", which in turn depends on the speed of forewing closure and file teeth distribution. The second step of the sound production consists of the interaction of the source signal with the membrane of both forewings, the filter, acting as a mechanical resonator [17]. The resonant properties of the left forewing, particularly of specific cells defined as the harp and the mirror, amplify the energy of the source signal and radiate the sound [18,19] (Fig. 1B–C).

Studies have shown that the harmonic-dominant signals produced by Lebinthini crickets are not simply due to evolution of morphological (e.g., higher teeth density along the stridulatory file) and behavioural (e.g., higher speed of forewing motion) traits enabling an increased tooth-strike rate during the stridulation step [20]. The measured tooth-strike rate in these species, the dominant frequency of the vibrational source signal, corresponds to the non-dominant fundamental frequency of the calling song. Based on this knowledge, the cause of the harmonic amplification in the songs of Lebinthini crickets is likely due to changes in the resonant properties of the forewings (the filter) i.e., during the second step of the sound-production mechanism.

We tested this hypothesis by studying two species of Eneopterinae crickets representing both situations: one species with a low-frequency song outside the Lebinthini tribe, and one Lebinthini species producing high-frequency, harmonic-dominant songs. The first species investigated, *Nisitrus malaya* Robillard & Tan, 2021, belongs to the tribe Nisitrini (Gryllidae, Eneopterinae). Its calling song is characterised by a dominant fundamental frequency (~7.0 kHz) that matches the acoustic spectral structure of sounds produced by the well-studied Gryllinae crickets [21] (Fig. 1C). The song also contains several well-amplified harmonic frequencies, which differs from the songs of the gryllines, where most of the acoustic energy is concentrated in a narrow-band, pure tone signal centred on the fundamental frequency [17]. Based on the phylogenetic position of *N. malaya* and the spectral characteristics of its calling song, no harmonic-hopping event has occurred during the evolutionary history of this species, making it an ideal candidate species to compare with a species of the tribe Lebinthini (Fig. 1B). The second species we studied is *Ponca hebardi* Robillard, 2005, a member of the Lebinthini tribe whose calling song is characterised by a dominant frequency (~18 kHz) corresponding to the third harmonic of the fundamental frequency [22]. Phylogenetic studies concluded that the calling song of *P. hebardi* arose because of a harmonic-hopping event that occurred at the base of the Lebinthini tribe [13] (Fig. 1A).

We first used the finite element method and computed tomography imaging to build realistic finite element models (FEM) of the forewings of the two species to reproduce their vibro-acoustic properties and mechanical behaviour. We used results from Laser Doppler Vibrometry (LDV) studies on forewings of real specimens of both species to calibrate and test the validity of our models. We investigated the role of structural and physical parameters on the behaviour of the models by studying the effect of their variation. A comparison of the two models highlighted the differences between the two species. Two different types of geometries were used in the study of the vibro-acoustic behaviour of the forewings. The first one, modelling the forewing membrane as a perfectly flat plate, allowed us to faithfully reproduce the resonant response of the low-frequency species *N. malaya*, but showed several limitations on the high-frequency species *P. hebardi*. To refine the model of this second species, we used morphological landmarks measured on a real specimen to integrate the 3D structure of the forewing to the FEM geometry, building a real 3D geometry. Our results show that the production of amplified harmonic frequencies in the songs of Lebinthini crickets depends on different biophysical parameters. Firstly, our results suggest that forewing venation plays an important constraining role that distinguishes the resonant response of forewings between low-frequency and high-frequency calling species. In addition, we show that both the 3D structure and the damping properties of the forewing membrane play a significant role in the production of amplified high frequencies in the vibro-acoustic behaviour of *P. hebardi*. Finally, we discuss the implications of our modelling results regarding the evolutionary origin of the harmonic amplification mechanism of Lebinthini crickets, and compare it to that described in bee-hummingbirds [3].

2. Materials and Methods

2.1. Taxonomic sampling

The first species investigated, *Nisitrus malaya,* belongs to the tribe Nisitrini (Gryllidae, Eneopterinae), whose calling songs are characterised by a dominant fundamental frequency (~7.0 kHz) that match the acoustic spectral structure of sounds produced by the well-studied Gryllinae crickets [21]. However, the song of this species also contains several well-amplified harmonic frequencies, which distinguishes it from the songs of the majority of cricket species, where most of the acoustic energy is concentrated in a narrow-band, pure tone signal centred on the fundamental frequency [17]. The presence of such high-amplitude harmonic frequencies in the calling songs of many Eneopterinae crickets is considered to be an acoustic characteristic of the whole subfamily [15]. However, as in the case of *N. malaya*, the presence of amplified harmonic components does not necessarily correlate with harmonic-dominant signals, and phylogenetic studies have suggested that harmonic-hopping occurred more recently and several times in the evolutionary history of Eneopterinae crickets, the most important one being at the time of the emergence of the Lebinthini tribe [13] (Fig. 1). The phylogenetic position and the spectral characteristics of the calling song of *N. malaya* made it an ideal candidate species to create a model to compare with that of a species of the tribe Lebinthini (Fig. 1).

Males of *N. malaya* emit calling songs composed of bouts of variable length, made of short echemes consisting of triplets of syllables [21]. The spectrum of the call consists of a series of harmonics with three distinct peaks, the first (the fundamental frequency) being the

dominant frequency of the song at about 7.35 ± 1.28 kHz (6.20–9.39 kHz), followed by two harmonics peaking at 13.33 ± 1.01 kHz (12.23–15.07 kHz) and 18.88 ± 0.77 kHz (17.23–20.07 kHz) respectively.

The second species we modelled is *Ponca hebardi* Robillard, 2005, a member of the Lebinthini tribe. Its calling song is composed of a single syllable with an average duration of 51.2 ± 8.6 ms [22]. The dominant frequency of the song has a value of 17.6 ± 0.3 kHz, which corresponds to the third harmonic peak. Phylogenetic studies suggested that the calling song of *P. hebardi* arose because of a harmonic-hopping event that occurred at the base of the Lebinthini tribe [13] (Fig. 1).

2.2. Laser Doppler vibrometry

Wing-resonance recordings from previous LDV studies [23] were used as reference for *N. malaya*. Forewing resonance was measured on four live males coming from field collection in Singapore, using a micro-scanning LDV (Polytec PSV-300-F; Polytec GmBH, Waldbronn, Germany) at the University of Bristol, UK, with an OFV-056 scanning head. The position of the laser spot on the wing membrane was monitored by a live video feed to the vibrometer controller and data management computer. Male crickets were mounted on a silicone holder using metal clamps to secure the legs, and the forewings were extended laterally by fixing the axillary sclerites with beeswax [24]. Both tegmina were measured with 250–300 laser scanning points and their vibrations were studied in response to broadband acoustic stimulation (periodic chirp) from 1 to 50 kHz at a corrected and flattened stimulation level of 80 ± 0.3 dB. Acoustic signals were generated by the internal data acquisition card of the PSV 300, amplified and transmitted from a loudspeaker located 11 cm behind the specimen.

One dry specimen of *P. hebardi* from the collections of the Muséum national d'Histoire naturelle (MNHN) was transported to the University of Lincoln, UK, for LDV study. After being relaxed in a humid chamber for 72 h, forewings resonances were measured and recorded using a PSV-500 LDV and PSV software v.9.1. Experiments were carried out in an anechoic chamber where forewings were acoustically stimulated using broadband periodic chirps ranging from 2 to 50 kHz. Playback of stimuli was controlled via the PSV-500 control box, delivered via a loudspeaker (Avisoft Vifa, Avisoft Bioacoustics, Glienicke, Germany) and monitored using a calibrated 1/8″ Brüel & Kjær type 4138 microphone, connected to a preamplifier (type 2633) and amplifier (type 5935L; all Brüel & Kjær, Nærum, Denmark). Measurements were performed in the frequency domain, using 390–410 measurement points per forewing, a sample rate of 128 kHz, 6400 NFFT lines and averaging over 5 measurements per point [23].

2.3. CT-scans of the forewings

Computed tomography (CT) datasets have been acquired at the biomedical beamline ID17 of the European Synchrotron Radiation Facility. The beamline is fed by two wiggler x-ray sources. The beam, for these measurements, has been monochromatized at a 35 keV energy by a double Laue monochromator before reaching the sample stage. Each tomographic acquisition consisted of 2000 angular projections acquired continuously over a 180-degree range with an integration time of 0.1 s per angular projection. The propagation-based phase contrast technique has been used as image contrast mechanisms. For the data acquisition, an indirect detection optics consisting in a LuAG:Ce scintillator screen coupled with 10x magnification lens and a PCO edge 5.5 sCMOS camera leading to an image pixel size of 0.7 μm, was employed [25]. The CT datasets were successively reconstructed using the Filtered Back Projection algorithm implemented in the PYHST2 package [26].

2.4. "Flat FEM" geometry

We choose to model the regions of the male cricket forewings that are actively involved in vibration, i.e., the dorsal area between the inner forewing boundary (bearing the plectrum) and the boundary delimited by the anterior cubital vein (Fig. S7). The forewings of several cricket species are known to be asymmetric, either in terms of morphology, physical properties or the way the forewings are mechanically excited [17]. Due to these differences, the two forewings may vibrate and generate sound differently from each other. In these cases, the "acoustically active" forewing, responsible for most of the acoustic signal generated by the system, is usually the left forewing, as it receives the mechanical energy through the plectrum [24]. Although no obvious morphological differences seem to exist between the right and left forewings in Lebinthini, some differences in their vibro-acoustic behaviour could still be observed in vibrometric studies [23]. Therefore, we modelled the left forewings for both our focal species.

The open-source vector graphics editor Inkscape (Inkscape Project, inkscape.org) was used to construct a two-dimensional layer representing the outline and venation pattern of the forewings of the two species studied. Two high-resolution photographs of the flattened forewings were taken with a stereomicroscope Leica MZ16 (Leica Microsystems GmbH, Wetzlar, Germany) connected to an AmScope MU1000 digital camera (www.Amscope.com), then imported in Inkscape as a basis to draw the layers (Fig. S7). Layers were exported to Drawing eXange Format (.dxf), then imported into the commercial finite element modelling software COMSOL Multiphysics® (COMSOL Multiphysics® v. 5.5, Comsol, Inc., Burlington, MA, USA) as a two-dimensional geometry (Fig. S7). We used the Structural Mechanics and Acoustics modules of COMSOL as the main tools to model the physical properties and simulate the vibro-acoustic behaviour of the forewings.

A semi-3D model of each forewing was built in COMSOL, consisting of a 2D representation of the forewing membrane and veins to which specific material properties and thickness values were assigned using shells to model the forewing membrane and beams to model the veins. The veins were modelled either as solid circular beams with thickness values assigned corresponding to the total diameter of the veins (d_o), or as hollow pipes, with a second value d_i derived from vein wall thickness ($d_i = d_o$-2*wall thickness).

Thickness values are measured from high-resolution 3D images of both forewings, previously reconstructed from CT scans. The

Amira software (v. 6.7.0, Thermo Fisher Scientific) was used to reconstruct a 3D forewing geometry from the 2D CT images, and colour-coded "thickness maps" (Fig. S7) were generated using the "Surface Thickness" module of the software. Thicknesses values were then assigned to the different forewing regions and veins based on these coloured maps (Fig. S7). When modelling veins as hollow pipes, additional measurements of the outer diameter d_o of the veins were taken under the stereomicroscope by measuring the visible width of the veins. The final venation pattern for both species consisted of solid and hollow veins, depending on the measured difference between the thickness value obtained from the scans, and the measured outer diameter.

2.5. "3D FEM" geometry

The general 3D structure of the left forewing of *P. hebardi* was determined using ten landmarks, described in Table S3 and shown in Fig. S8. These landmarks characterise key structures involved in cricket song production: the file, the harp and the mirror. Eight landmarks are type I landmarks corresponding to homologous intersections of veins. The remaining two landmarks correspond to one type II landmark corresponding to the end of curvature the vein carrying the stridulatory file (vein 1A), and one type III landmark corresponding to the projection of the landmark 1 on the CuA vein. Landmark data were obtained using a MicroVu Vertex 251 and Inspec software for the left forewing of three male specimens from the MNHN.

The 3D coordinates of the landmarks were imported into COMSOL, then integrated with the flat geometries of the former finite element models in order to obtain geometries that deform in the 3 dimensions. To do so, a bilinear interpolation function was created in COMSOL, taking the (x,y,z) coordinates of the landmarks as the points of the function being interpolated, the x and y coordinates being the two variables of the function (Fig. S9). A parametric surface was then created, i.e. a 3D surface whose coordinates are defined using parameters. The values of the x and y fields coordinates were defined as intervals covering the forewing area. The values of the z field coordinates of the surface were defined to correspond to the values of the interpolation function. In this way, a 3D surface was created that incorporates the 3D coordinates of the landmarks.

2.6. Meshing

The geometries created were meshed in COMSOL using free triangular elements. The mesh for the *N. malaya* model comprised 3210 elements, with a minimum element size of ~2.17 μm, a maximum of ~217 μm, and an average element quality of ~0.81 (taking skewness as the quality measure). The mesh for the *P. hebardi* flat FEM comprised 3773 elements, with a minimum element size of ~2.76 μm, a maximum of ~276 μm, and an average element quality of ~0.80. The mesh for the *P. hebardi* 3D FEM comprised 5078 elements, with a minim element size of ~2.75 μm, a maximum of ~275 μm, and an average element quality of ~0.80.

2.7. Rayleigh damping coefficients calculation

In order to model the damping of the membrane of the models, the Rayleigh damping method was used. Rayleigh damping models the damping as:

$$c = \alpha_{dM} \cdot m + \beta_{dK} \cdot k \tag{1}$$

where α_{dM} and β_{dK} are the mass- (m) and the stiffness- (k) proportional Rayleigh damping coefficients, respectively. α_{dM} is expressed in s^{-1} and β_{dK} in s.

Both coefficients are related to the damping ratio ζ_i, a dimensionless measure how rapidly the oscillations in a system decay after a disturbance. This relation is expressed as:

$$\zeta_i = \frac{\alpha_{dM}}{2\omega_i} + \frac{\beta_{dK} \cdot \omega_i}{2} \tag{2}$$

where $\omega_i = 2\pi f_i$, and is the natural frequency at resonant node *i*.

Using two damping ratios ζ_1 and ζ_2 and their corresponding frequencies f_1 and f_2, the mass- and stiffness-proportional coefficients can be calculated for the model using the following relationships:

$$\alpha_{dM} = 4\pi f_1 f_2 \cdot \frac{\zeta_1 f_2 - \zeta_2 f_1}{(f_2)^2 - (f_1)^2} \tag{3}$$

$$\beta_{dK} = \frac{\zeta_2 f_2 - \zeta_1 f_1}{\pi \cdot \left((f_2)^2 - (f_1)^2\right)} \tag{4}$$

The damping ratios ζ_1 and ζ_2 were approximated from the experimental data of the LDV measurements of both species. The quality factor of two resonant peaks was obtained from the LDV measurements as:

$$Q = \frac{f_i}{\Delta f} \tag{5}$$

where f_i is the frequency value of the resonant peak *i*, and Δf is the resonance width or full width at half maximum (FWHM) i.e. the

bandwidth over which the power of vibration is greater than half the power at the resonant frequency, measured at most −3 dB of attenuation.

The damping ratio ζ_i given the quality factor Q_i is then approximated by:

$$\zeta_i = \frac{1}{2Q_i} \tag{6}$$

Mass- and stiffness-proportional Rayleigh damping coefficients were measured from LDV measurements for the harp and mirror region, and for the rest of the forewing taken as a whole. The vibro-acoustic response data of the forewings obtained from LDV were expressed as displacement of the forewing membrane as a function of the excitation frequency. These data were converted in dB using the following relationships:

$$dB_d = 20\ log_{10}\left(\frac{d}{d_{ref}}\right) \left| d_{ref} = 10^{-12} m \right| \tag{7}$$

The resonant peaks chosen for measuring the damping coefficients were the two peaks showing the highest amplitude in the frequency range between 6 kHz and 23 kHz. The calculated damping parameters were then integrated into the FEM, at the Shell and Beam interfaces modelling the forewing membrane and veins respectively.

2.8. General model parameters

Physical material property values were assigned to the different forewing regions and veins by drawing on different literature sources. Three essential parameters values had to be determined: the material density *rho*, the Poisson's ratio *nu*, and the Young's modulus *E*. Several studies of insect cuticle from the literature provided information on the values of these three parameters, which depend mainly on the type of cuticle composing the part of the insect studied. The density of the cuticle remains fairly constant, ranging from 1000 to 1300 kg/m^3, while the Young's modulus can have a wide range of values from 100 MPa to at least 50 GPa [27, 28]. Young's modulus of the forewings of the two species studied, as well as that of all cricket and locust wings, is not known. However, previous studies suggested that the Young's modulus of cricket wings should be between 1 and 10 GPa [27]. Therefore, the Young's moduli of the forewing veins and membrane were treated as unknowns and their variations were examined in the models to determine

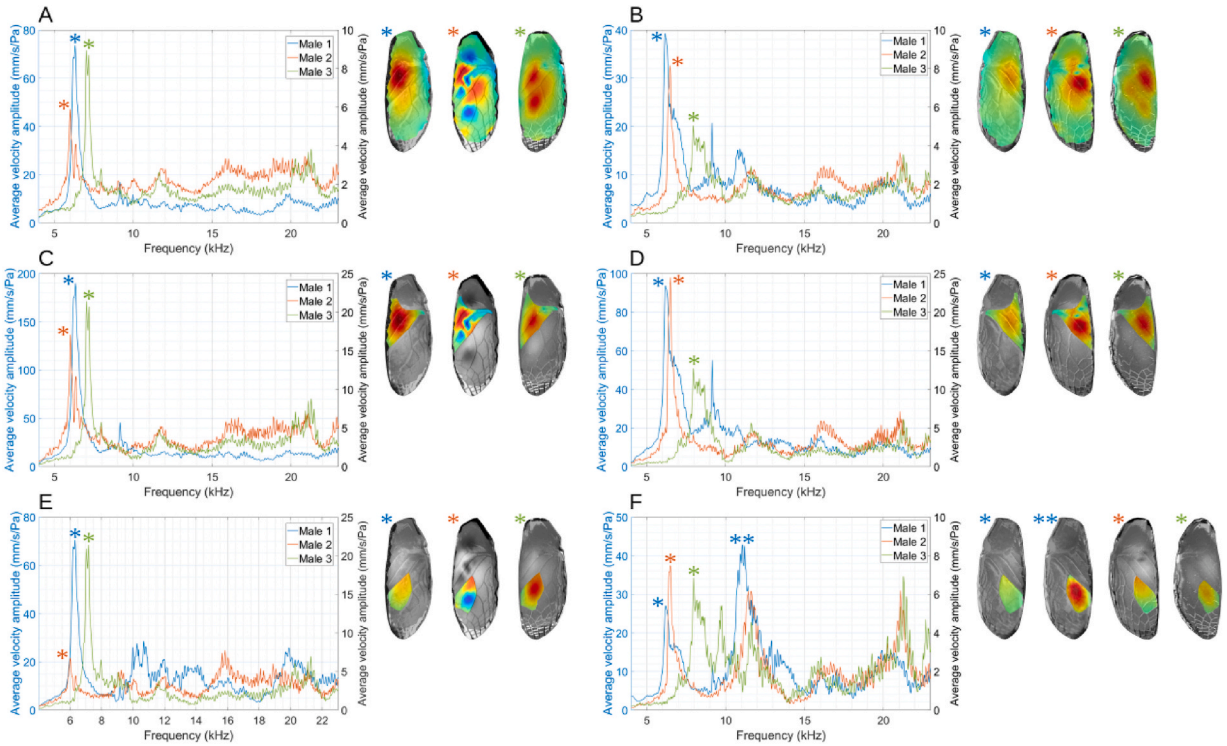

Fig. 2. Resonant response of real forewings of *Nisitrus malaya*. A-B Frequency response spectrum of the whole forewing of the left (A) and right (B) forewing of three male specimens of *N. malaya* measured with LDV. C-D Frequency response spectrum of the harp region of the left (C) and right (D) forewing of the three males. E-F Frequency response spectrum of the mirror region of the left (E) and right (F) forewing of the three males. A-F The velocity maps of the resonant modes corresponding to the resonant peaks marked by asterisks for each panel are shown in inserts. Phase maps of the resonant modes can be found in Fig. S2.

the values that matched the vibro-acoustic behaviour of the models with LDV studies in terms of frequency range. The density of the forewing cuticle was set at 1200 kg/m^3 and the Poisson's ratio at 0.33 [29]. A fixed constraint, i.e. displacements are zero in all directions on the selected boundaries, was applied to the boundaries corresponding to where the forewings are attached to the second segment of the thorax, and along the anterior ulnar vein, representing the missing lateral field constraint.

2.9. Behaviour of vibro-acoustic models in the frequency domain

The eigenfrequencies and eigenmodes of the models were calculated using the "Eigenfrequency" study type in COMSOL. To calculate the vibro-acoustic behaviour of the models in the frequency domain, the "Frequency Domain" study type was used. The models were excited at frequencies between 1 and 30 kHz (in 100 Hz steps) and the excitation was applied as a normal 1 Pa load over the entire forewing surface (face load). The results were examined in the frequency range corresponding to that of the calling songs (between 6 and 23 kHz) by calculating the velocity amplitude and the total displacement of the membrane as a function of the excitation frequency. For each model, the resonant response of the whole forewing was calculated, along with the specific resonant response of the harp and mirror regions. These results were compared to the resonant response of the same areas in the LDV results. The most fitting set of stiffness parameters for each model was chosen according to the resonant response measured on real specimens of the corresponding species. Similar resonant frequencies between LDV and FEM results were determined according to the number of nodes and antinodes, along with their relative position in the different regions of the forewing. The frequency values of the resonance peaks in the frequency domain were considered to correspond to the LDV measurements when they were within ±1 kHz of the mean value measured experimentally.

3. Results

3.1. Calling song fundamental and dominant frequency

Males of *N. malaya* emit calling songs composed of bouts of variable length, made of short echemes consisting of triplets of syllables [21]. The spectrum of the call consists of a series of harmonics with three distinct peaks, the first (the fundamental frequency) being the dominant frequency of the song at about 7.35 ± 1.28 kHz (6.20–9.39 kHz), followed by two amplified harmonics peaking at 13.33 ± 1.01 kHz (12.23–15.07 kHz) and 18.88 ± 0.77 kHz (17.23–20.07 kHz) respectively. LDV data from three males were analysed to study the resonant response of the forewings of *N. malaya*. Fig. 2 shows the frequency response spectrum of the left (LW; Fig. 2A, C and 2E) and right (RW; Fig. 2B, D and 2F) forewings of the three specimens, while Table 1 summarises key parameters values measured from LDV results.

The calling song of *P. hebardi* is composed of a single syllable with an average duration of 51.2 ± 8.6 ms [22]. The dominant frequency of the song has a value of 17.6 ± 0.3 kHz, which corresponds to the third harmonic peak.

3.2. Forewing resonance measured using LDV

The forewings of the three measured specimens of *N. malaya* present a similar vibro-acoustic behaviour in the frequency domain, both for the LW and RW. However, the resonant response of male 1 have an amplitude range several times higher than the responses of male 2 and 3, around eight times higher for the LW and four times higher for the RW. Also, the response of the LW have an amplitude range around two times that of the RW for male 1, while the responses of the two forewings have similar amplitude range for the two

Table 1
Frequency value and velocity amplitude of the dominant resonant peak of different regions of the left and right forewing of the three male specimens of *N. malaya* as measured with LDV.

Specimen	Forewing	Region	Dominant peak's frequency	Dominant peak's amplitude
Male 1	LW	Entire forewing	6320 Hz	~73.70 mm/s/Pa
		Harp	6320 Hz	~190 mm/s/Pa
		Mirror	6320 Hz	~70.50 mm/s/Pa
	RW	Entire forewing	6200 Hz	~39.30 mm/s/Pa
		Harp	6200 Hz	~93.8 mm/s/Pa
		Mirror	11060 Hz	~42.9 mm/s/Pa
Male 2	LW	Entire forewing	6000 Hz	~5.90 mm/s/Pa
		Harp	6000 Hz	~17.10 mm/s/Pa
		Mirror	15844 Hz	~7.73 mm/s/Pa
	RW	Entire forewing	6500 Hz	~8.17 mm/s/Pa
		Harp	6500 Hz	~24.5 mm/s/Pa
		Mirror	6469 Hz	~7.5 mm/s/Pa
Male3	LW	Entire forewing	7031 Hz	~8.95 mm/s/Pa
		Harp	7031 Hz	~21.40 mm/s/Pa
		Mirror	7187 Hz	~21.40 mm/s/Pa
	RW	Entire forewing	7969 Hz	~5.05 mm/s/Pa
		Harp	7969 Hz	~12.7 mm/s/Pa
		Mirror	21281 Hz	~6.92 mm/s/Pa

other specimens. The response of the LW shows a dominant resonant peak between 6.0 and 7.1 kHz, close to the dominant frequency of the calling song. The resonant mode of the forewing membrane associated with this dominant peak varies slightly in shape between the three specimens. It globally shows a large area of the LW, including the harp, the mirror and a large part of the basal region, vibrating in phase, although this shape appears more complex in the response of male 2. The harp region appears to be the main resonant region of the forewing at this frequency for male 1 and 2, while male 3 shows a contribution of both the harp and mirror regions.

The response of the RW shows a dominant resonant peak between 6.2 and 8.0 kHz, also in the range of the fundamental frequency of the calling song. The resonant mode associated with this dominant peak appears of similar shape in the results of the three measured males, mainly consisting of one large antinode spending over the harp and mirror regions, as well as on a large part of the chords and anal region. The harp region is the main resonant region at this frequency in the three specimens' results. By looking at the resonant responses of the mirror region for the three specimens, we can see that this region present high-amplitude resonant peaks of higher frequency than that of the dominant peak seen in the response of the RW as a whole. The mirror region of male 1 shows a dominant resonant peak at 11.06 kHz, while male 3 present a co-dominance of two peaks, one at 7.97 kHz (amplitude of 6.84 mm/s/Pa), and the other at 21.28 kHz (amplitude of 6.92 mm/s/Pa).

The resonant response of the forewings of one male specimen of *P. hebardi* have been measured using LDV. Fig. 4 shows the frequency response spectrum of the RW and LW of the measured specimen. Table 2 summarises key parameters values obtained from LDV results. Although the LW and the RW show similar vibro-acoustic behaviour in the frequency domain, the resonant response of the LW is about 2 times greater in amplitude than that of the RW. The LW shows a dominant resonant peak at 21.15 kHz (Fig. 4A), above the dominant harmonic frequency of the species' calling song [22]. The region of maximum velocity amplitude is clearly the mirror, making it the main resonant region of the forewing at this frequency. Although of little amplitude, a second resonant peak can be observed at 7.90 kHz, above the fundamental frequency of the calling song. Although the region of maximum velocity amplitude is again the mirror (Fig. 4E), we can see that the harp region also contributes strongly to the overall resonance of the forewing at this frequency (Fig. 4C). If we examine the resonant responses of the harp and mirror regions separately, we can see that the two regions contribute differently to the general vibro-acoustic behaviour of the LW (Fig. 4C and E). The harp region shows a dominant resonant peak at 21.25 kHz very close to that of the LW as a whole. Three other resonant peaks are visible. The first and second are found at 7.53 kHz and 8.48 kHz, close to the peak at 7.9 kHz in the general response of the LW. The third is found at 12.28 kHz, not found in the response of the LW as a whole, although close in amplitude (~6.31 mm/s/Pa) to the dominant peak seen at 21.25 kHz (~6.71 mm/s/Pa). The resonant response of the mirror is very similar to the general response of the LW, with a dominant peak found at 21.14 kHz, along with another one at 7.9 kHz. However, the amplitude range of the mirror region is about twice that of the harp, confirming that it is the main resonant region of the forewing.

The RW shows a dominant resonant peak at 21.14 kHz, the same frequency as the dominant peak of the LW (Fig. 4B). As for the LW, the main resonant region of the forewing at this frequency appears to be the mirror. Three other resonant peaks are visible in the response of the RW. A first is found at 5.39 kHz, a second at 8.66 kHz, and a third at 13.98 kHz. The mirror region appears to be the main resonant region at 8.66 kHz, while it is the harp region for the peak at 13.98 kHz. Examining the responses of the harp and mirror regions separately (Fig. 4D and F), we see that the two regions contribute differently to the general vibro-acoustic behaviour of the RW. The harp region shows a dominant resonant peak 14.31 kHz, close to the peak found at 13.98 kHz in the general response. Among several other resonant peak of little amplitude, one peak is found at 5.39 kHz, corresponding to the one present in the general response, and another is seen at 21.14 kHz, at the same frequency of the dominant resonant peak of the RW as a whole. The mirror region shows a dominant resonant peak at 21.14 kHz, like in the general response of the LW. Several other resonant peaks are visible in the spectrum, including one at 8.66 kHz which correspond to the peak found at the same frequency in the response spectrum of the whole forewing.

3.3. Vibro-acoustic behaviour using flat FEM

A FEM of the LW of *N. malaya* have been constructed to reproduce the results measured during LDV studies. Forewing's geometry has been faithfully reproduced based on high-resolution photographs of the dorsal field of the forewing of a real specimen. Thickness of the forewing's membrane and veins was set for the different regions based on values from CT-scans of a real specimen. Boundary conditions of the FEM were defined using a fixed constraint applied along the anterior ulnar vein, representing the missing lateral field, and on the basal extremity of the forewing, representing the attachment to the thorax. Damping was modelled using mass- and stiffness-proportional Rayleigh damping coefficients. These coefficients were estimated using data from the LDV study of the forewing of male specimen 3, for three different regions of the forewing: the harp, the mirror, and the rest of the forewing (see Table S1). Finally,

Table 2
Frequency value and velocity amplitude of the dominant resonant peak of different regions of the left and right forewing of the male specimen of *P. hebardi* as measured with LDV.

Forewing	Region	Dominant peak's frequency	Dominant peak's amplitude
LW	Entire forewing	21150 Hz	~4.00 mm/s/Pa
	Harp	21250 Hz	~6.70 mm/s/Pa
	Mirror	21150 Hz	~13.90 mm/s/Pa
RW	Entire forewing	21140 Hz	~2.70 mm/s/Pa
	Harp	14310 Hz	~4.20 mm/s/Pa
	Mirror	21140 Hz	~8.60 mm/s/Pa

essential physical properties values, i.e. density *rho*, Poisson's ratio *nu*, and Young's modulus *E*, were defined based on studies found in scientific litterature. For more details about the FEM construction, please refers to the Materials and Methods section. On the three physical properties used in the FEM, Young's modulus (E) was the only one which value was highly variable across insect species and cuticle types. As the variation in stiffness properties in cricket forewings was poorly studied, a sensitivity analysis of this parameter for both the forewing's membrane (E_m) and veins (E_v) was then conducted (Fig. S1).

The resonant response of the FEM was studied between 5 and 23 kHz, a frequency range corresponding to that of the calling song of the species [21]. The variation of E_m value causes shifts in both frequency and amplitude of the resonant peaks (Fig. S1A–S1B). The higher the E_m value, the higher the values of the resonant frequencies. However, a variation of this parameter has no effect on the shapes of the resonant modes. A frequency range matching the frequency values of the dominant resonant peak measured in LDV responses was found for E_m values between 7 GPa and 13 GPa (Fig. S1B). For stiffness values in this range, the dominant resonant peak of the FEM is located between 6.2 kHz and 8.4 kHz, which corresponds to the resonant frequency range of real forewings (6.9 $\pm$ 0.68 kHz for LW) [23].

Varying E_v value results in a similar, albeit less pronounced, shift in frequencies of the resonant peaks than that observed when E_m value is varied by the same proportion (Fig. S1C–1D). However, changing forewing's venation stiffness also affects the shapes of the resonant modes associated with the peaks. Keeping a fixed E_m value of 10 GPa, a shift in the E_v value from 1 GPa to 100 GPa results in an increase in the value of the dominant resonant peak frequency of the forewing from 7.4 kHz to 10.2 kHz. As the stiffness of the veins increases, the point of maximum amplitude of the resonant mode becomes more confined to the centre of the harp (Fig. S1C), although the shape of the mode seems not strongly affected.

Fig. 3 shows the vibro-acoustic response of the best-fitting FEM compared to measured LDV data, i.e. with a E value similar for the membrane and the venation, of 10 GPa. The dominant resonant peak is found at 7.4 kHz. The resonant mode associated with this peak is close to that observed in LDV results of males 1 and 3 for the dominant resonant peak. The amplitude of the dominant resonant peak is of ~5.3 mm/s/Pa (Fig. 3B), which is slightly below the amplitude of the dominant peak in the LDV response (Fig. 3A). Several other weakly enhanced resonant peaks are visible in the FEM response at higher frequencies, e.g at 8.2 kHz and around 15.1–15.2 kHz, associated with more complex resonant modes. The detailed observation of the response of the harp and mirror regions of the FEM

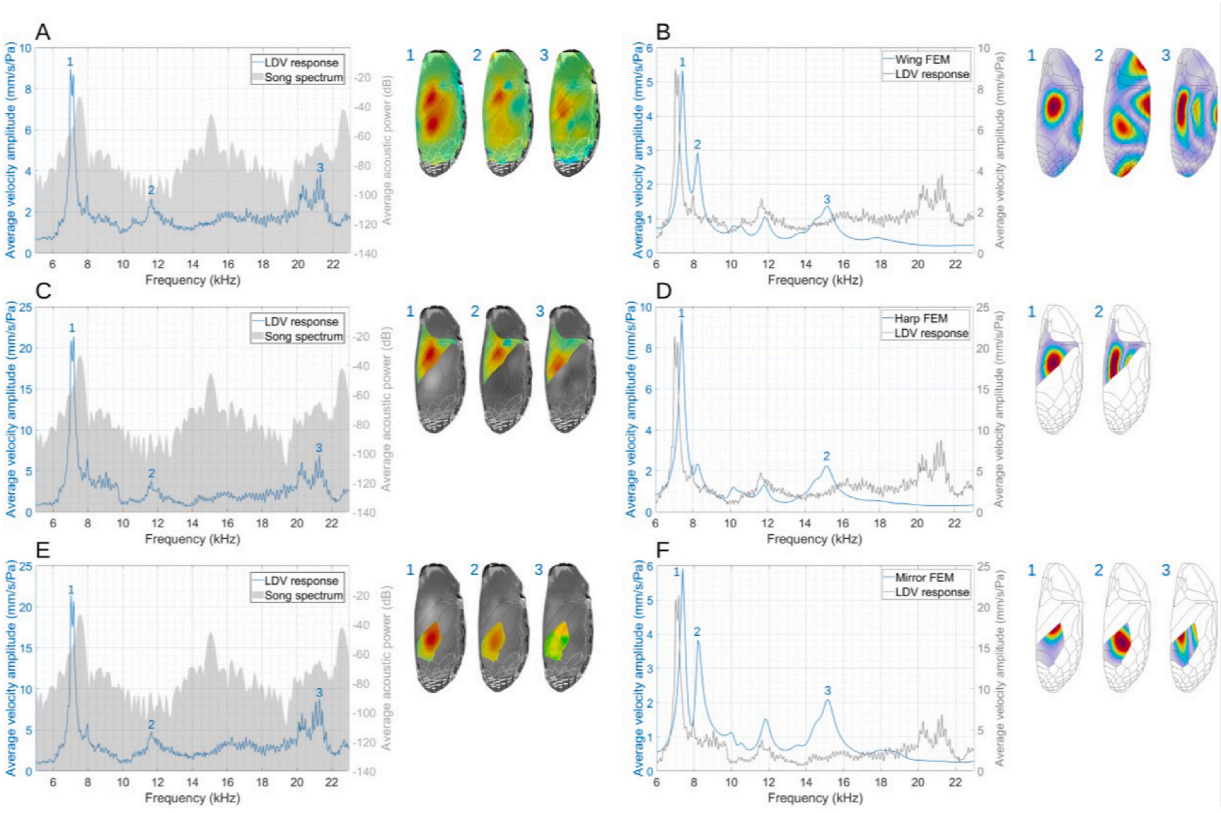

Fig. 3. Finite-element modelling of the resonant response of the forewing of *Nisitrus malaya*. Left: Frequency response spectrum of the forewing (A), harp (C), and mirror (E) of the *N. malaya* LW of male specimen 3 as measured by LDV (blue line) and acoustic amplitude spectrum of the recorded song of the measured individual (dark grey). Right: Frequency response spectrum of the forewing (B), harp (D) and the mirror (F) of the *N. malaya* FEM (blue line, Ev and Em = 10 GPa), and the corresponding response of the real LW of male specimen 3 as measured by LDV (grey line). A-F The velocity maps of the resonant modes corresponding to the resonant peaks marked by numbers for each panel are shown in inserts. Phase maps of the resonant modes can be found in Fig. S3.

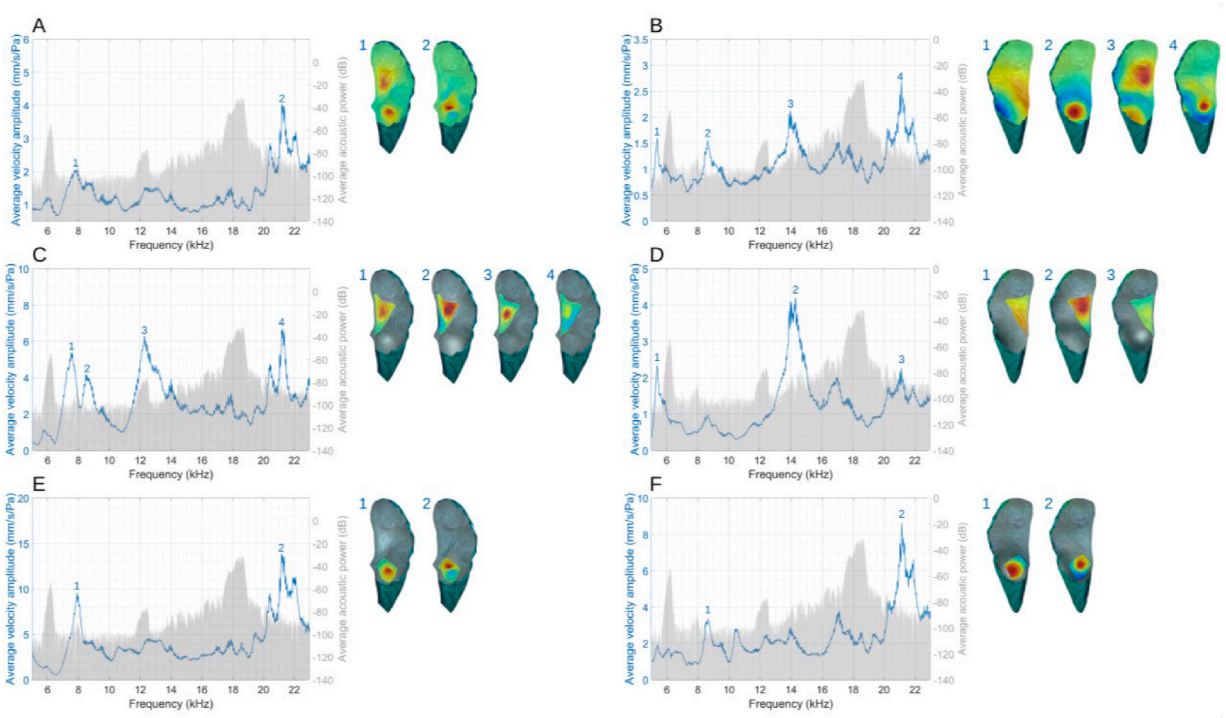

Fig. 4. Resonant response of real forewings of *Ponca hebardi*. A-B Frequency response spectrum of the whole forewing of the left (A) and right (B) forewing of the male specimen of *P. hebardi* measured with LDV. C-D Frequency response spectrum of the harp region of the left (C) and right (D) forewing of the male. E-F Frequency response spectrum of the mirror region of the left (E) and right (F) forewing of the male. A-F The velocity maps of the resonant modes corresponding to the resonant peaks marked by numbers for each panel are shown in inserts. Phase maps of the resonant modes can be found in Fig. S4.

(Fig. 3D and F) shows that the resonant peak at 8.2 kHz is more pronounced in the response spectrum of the mirror than in that of the harp. Velocity amplitude values indicate that the harp region seems to contribute more to the overall resonance of the forewing than the mirror. This is coherent with measured LDV data of males 1 and 2, although it seemed that the two regions contributed equally to the resonant response of male 3 (Fig. 3C and E).

Following the same methodology as for *N. malaya*, a FEM of the LW of *P. hebardi* was built (see Table S2 for measure of damping coefficients), and a sensitivity analysis of the E_m and E_v was conducted, aiming to reproduce the resonant response obtained in LDV study. The FEM response analysed was that of the dorsal field without the apical region, in order to study the same area as that measured with the LDV for this species. As for the *N. malaya* model, increases in Young's modulus of the membrane (E_m) and of the veins (E_v) affect the frequencies and relative amplitudes of the resonant peaks in the FEM response. The variation of E_v also has an effect on the shape of the modes associated with the resonant peaks in the response spectrum.

Eigenfrequencies studies showed resonant frequencies with mode shapes similar to those associated with the main resonant peaks in the LDV results by applying an E_v value several times higher than that of E_m. More precisely, we found that E_v value must be around forty times higher than E_m for the FEM to show resonant modes similar to those described in LDV results (Fig. 5). When this relation between E_m and E_v is applied, the FEM shows a resonant frequency with a mode shape similar with that of the peak found at 7.9 kHz in the LDV results. The region of maximum velocity amplitude for this resonant frequency is the mirror, and the basal part of the harp also contributes to the overall resonance. This resonant frequency of interest was labelled as f_a. When examining the other resonant peaks found in FEM response when the 1:40 ratio between E_v and E_m is applied, we see one whose mode shape is strongly similar to that of the dominant resonant peak in LDV results (Fig. 5). This second frequency of interest was labelled as f_b.

To bring f_a and f_b closer in the frequency domain to their relatives observed in the response of the real forewing, E_m was set at 2 GPa and E_v at 80 GPa, i.e. a ratio of 1:40 between the values of the two parameters. For this set of stiffness parameters, f_a is found at 7.2 kHz, close to the corresponding resonant peak at 7.9 kHz in LDV results. Resonant frequency f_b is found between 15.9 and 16.0 kHz, far below the frequency value of the corresponding dominant resonant peak (21.15 kHz) observed in LDV measures.

When examining the vibro-acoustic behaviour of this FEM in the frequency domain (Fig. 6) the dominant resonant peak of the response spectrum is found at 8.2 kHz, and is associated with a mode shape very similar to resonant frequency f_a, where the mirror appears to be the predominant resonant region of the forewing (Fig. 6A and B). Several additional well amplified peaks are visible at higher frequencies, e.g. at 15.6 kHz, where the mirror is again the main resonant cell, and at 18.6 kHz, where the harp carries most of the forewing resonance. All these peaks are associated with complex mode shapes, that are clearly different than that of resonant frequency f_b.

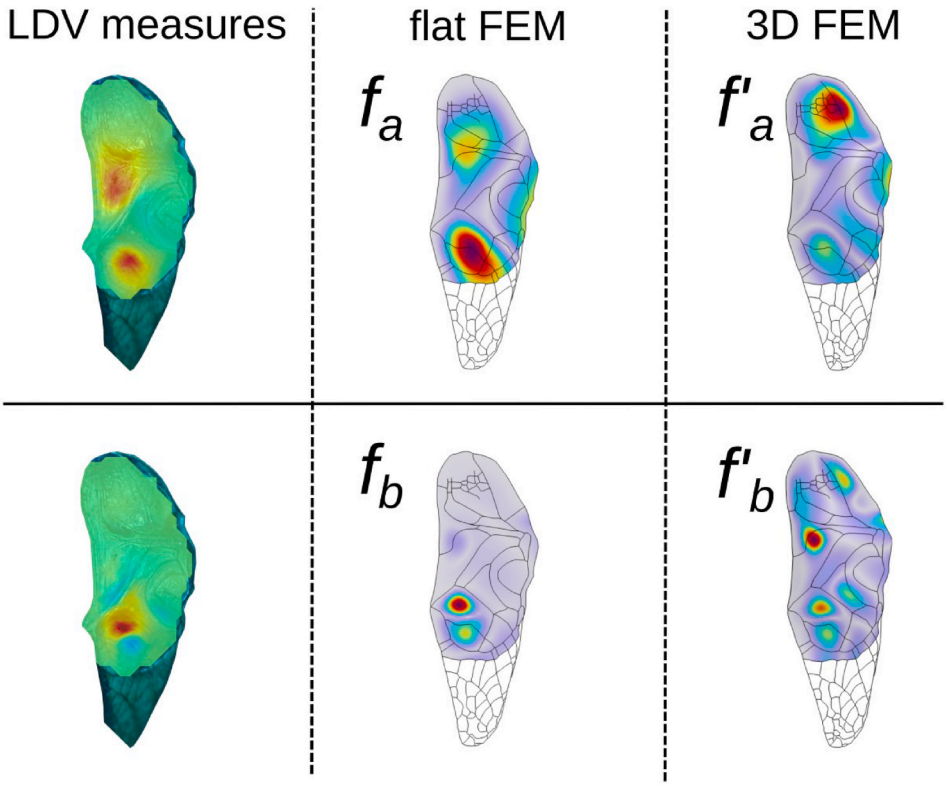

Fig. 5. Matching resonant frequencies in the flat and 3D FEM of *Ponca hebardi*. Up: Velocity maps of the resonant mode found at 7.9 kHz in the response spectrum measured with LDV (left), and corresponding resonant frequencies found in the flat FEM (centre, f_a) and 3D FEM (right, f'_a). Down: Velocity maps of the resonant mode found at 21.15 kHz in the response spectrum measured with LDV (left), and corresponding resonant frequencies found in the flat FEM (centre, f_b) and 3D FEM (right, f'_b).

Looking at the response of the harp and the mirror separately (Fig. 6D and F), we can see that the two regions have very different resonant responses, as in the LDV results (Fig. 6C and E). The vibro-acoustic behaviour of the harp (Fig. 6D) shows a dominant resonant peak of high frequency at 18.6 kHz, corresponding to the resonant peak found at this frequency in the response of the whole FEM. Two additional resonant peaks are visible at 8.1 kHz, corresponding to the dominant resonant peak seen in the whole FEM response, and at 13.4 kHz, corresponding to another little amplified resonant peak of the general response of the FEM. The vibro-acoustic behaviour of the mirror (Fig. 6F) shows a dominant resonant peak at 8.4 kHz close to the dominant peak of the general response. Another well amplified peak is found at 15.8 kHz, close to that seen at 15.6 kHz in the whole FEM. Furthermore, the poorly amplified peak at 18.7 kHz, corresponding to the well amplified peak at 18.6 kHz in the general response, show that the mode shape of the mirror at this frequency is very similar to that found both in resonant frequency f_b and in the mode shape associated with the dominant resonant peak in the response spectrum of the real forewing measured with LDV (Fig. 6E). Finally, the resonant response of the mirror is higher than that of the harp in amplitude, confirming that the mirror seems the dominant resonant region of the FEM vibro-acoustic behaviour.

3.4. Vibro-acoustic behaviour using 3D FEM

The resonant response of the flat FEM of *P. hebardi* showed several differences compared to that of the real forewing measured with LDV. In particular, respective amplitudes of the resonant peak in the response spectrum didn't follow what was observed experimentally (Fig. 6). We hypothesised that these discrepancies could be due to the high level of abstraction chosen for this FEM, with the forewing modelled as a perfectly flat plate. We tested this hypothesis by refining the geometry of the *P. hebardi* FEM to be closer to the reality. To do so, we measured 3D coordinates of key morphometric landmarks on the left forewing of three *P. hebardi* males in order to measure the overall 3D structure of the forewing. We integrated these 3D landmark coordinates into the FEM geometry to obtain a new 3D geometry, closer to the actual structure of the forewing of the species.

The 3D geometry also greatly affects the vibro-acoustic behaviour of the FEM of *P. hebardi* when looking at the resonant frequencies. Resonant frequencies close to f_a and f_b were found for E_v values around 20 times that of E_m (Fig. 5). When this set of stiffness parameters is applied, the 3D FEM show a resonant frequency, hereafter labelled f'_a, with a mode shape close to that of f_a, although being more complex. While this shape is similar to that of the mode found at 7.9 kHz in the real forewing response, the region of maximum velocity amplitude is not the mirror or the harp, but the anal region. Another resonant frequency, labelled f'_b, is found in the response of the 3D FEM, and its mode's shape seems close to that of f_b and of the dominant peak in the LDV response. The mirror is once

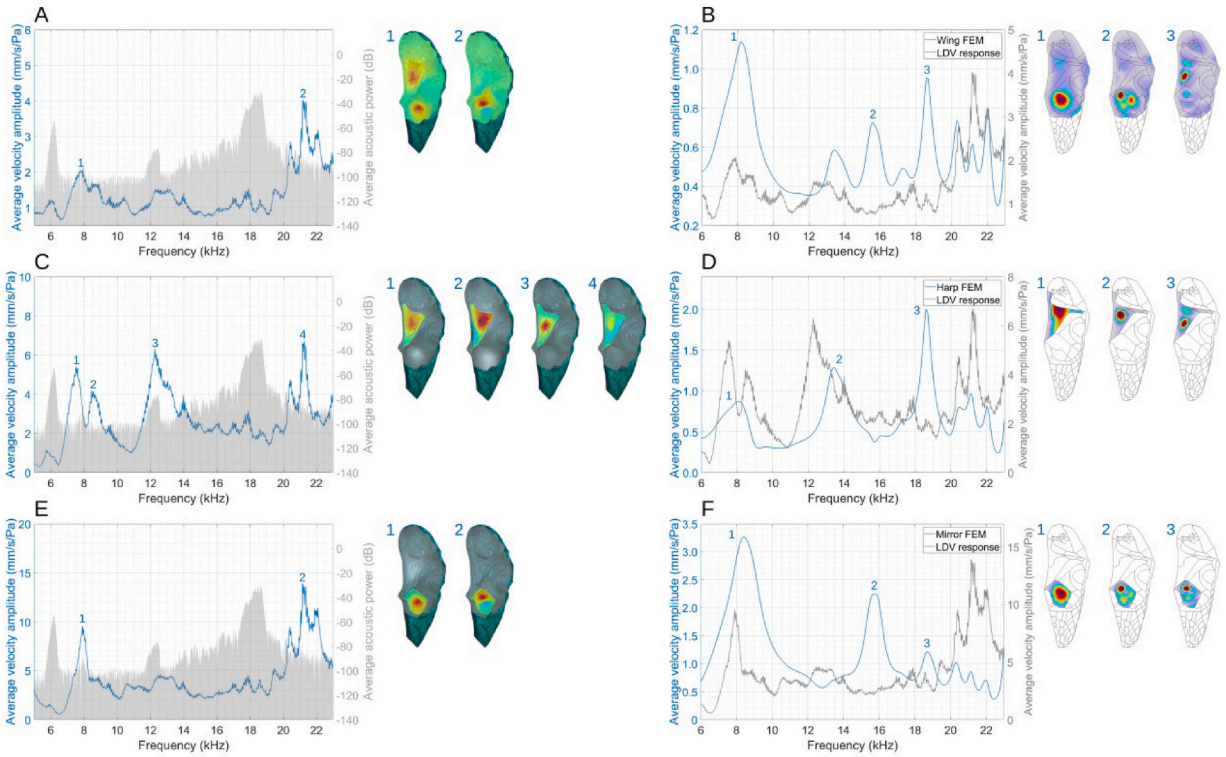

Fig. 6. Resonant response the flat FEM of *P. hebardi*. Left: Frequency response spectrum of the forewing (A), harp (C), and mirror (E) of the P. hebardi LW of male specimen measured with LDV (blue line) and acoustic amplitude spectrum of the recorded song of the individual (dark grey). Right: Frequency response spectrum of the forewing (B), harp (D) and the mirror (F) of the P.hebardi flat FEM (blue line, Ev = 80 GPa, Em = 2 GPa), and the corresponding response of the real LW measured with LDV (grey line). A-F The velocity maps of the resonant modes corresponding to the resonant peaks marked by numbers for each panel are shown in inserts. Phase maps of the resonant modes can be found in Fig. S5.

again one of the main resonant regions of the forewing at this frequency, but the harp also seems to play an important part in the overall resonance of the forewing.

When studying the vibro-acoustic behaviour of the 3D FEM in the frequency domain, a ratio of 1:20 was applied between the values of E_m and E_v (E_m was set at 1.5 GPa and E_v at 30 GPa) (Fig. 7A–C). With this set of values, a resonant frequency similar to f'_b is associated with the dominant resonant peak in the response spectrum at 18.8–18.9 kHz, a few kHz under the frequency value of the corresponding dominant resonant peak (21.15 kHz) observed in the LDV results (Fig. 7D). The region of maximum velocity amplitude at this frequency is the harp region, not the mirror region as it is seen in the resonant response of the real forewing measured with LDV. A second resonant peak is found at 7.8 kHz. It is associated with a resonant frequency resembling that found at 8.2 kHz in the flat FEM response, with the main resonating region of the forewing being the mirror.

The harp and the mirror still show very different resonant responses. The vibro-acoustic behaviour of the harp (Fig. 7B) shows a unique dominant resonant peak of high frequency, found at 18.9 kHz, corresponding to the dominant resonant frequency in the resonant response of the whole forewing. The vibro-acoustic behaviour of the mirror (Fig. 7C) shows a dominant resonant peak at 7.8–7.9 kHz corresponding to the second peak described in the spectrum of the forewing. Another well amplified peak is found at 18.8–18.9 kHz, corresponding to the dominant resonant frequency in the whole forewing response. In comparison with the results of the former flat FEM, we can see that the harp is now the region that participates the most to the dominant resonant peak observed in the resonant response of the whole forewing, while the mirror, although participating to the main resonant peak, is still mostly associated with the low frequency peak corresponding to the dominant peak in the flat FEM response.

4. Discussion

In most species of the tribe Lebinthini, the dominant frequency of the song corresponds to a harmonic frequency of the measured fundamental [e.g., [13]]. In the majority of (other) cricket species, the dominant frequency of the song is directly produced by the source of the sound-production mechanism. The source signal, i.e. the series of mechanical impulses generated by the periodic impact of each tooth of the stridulatory file, is conserved after being transmitted and amplified by the resonant membranes of the forewings. In Lebinthini species, the question arises as to whether the same mechanism acts to produce those dominant harmonic frequencies. While previous studies suggested that the interaction between the plectrum and the stridulatory teeth can constitute a source of

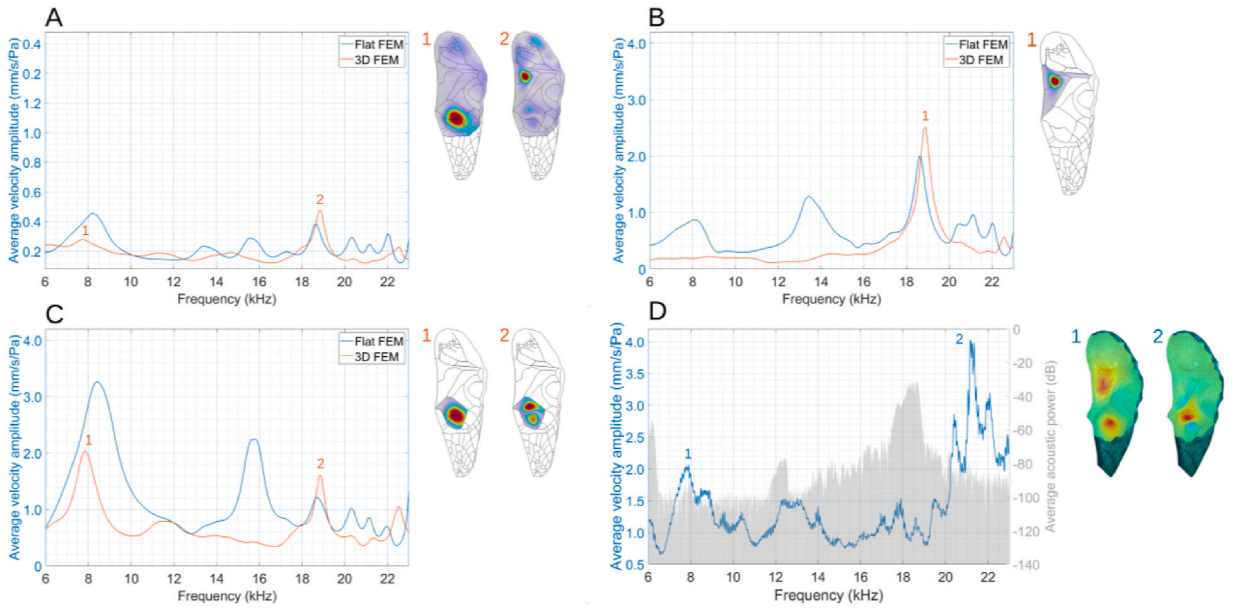

Fig. 7. Resonant response of the 3D FEM of *P. hebardi* compared with that of the flat FEM. A-C Frequency response spectrum of the dorsal field (A), harp (B), and mirror (C) of the 3D FEM (orange line, Em = 1.5 GPa, Ev = 30 GPa) and of the flat FEM (blue line, Em = 2 GPa, Ev = 80 GPa). D Frequency response spectrum of the forewing of the *P. hebardi* LW of male specimen measured with LDV (blue line) and acoustic amplitude spectrum of the recorded song of the individual (dark grey). A-D The velocity maps of the resonant modes corresponding to the resonant peaks marked by numbers for each panel are shown in inserts. Phase maps of the resonant modes can be found in Fig. S6

high-frequency components in the cricket song [30], previous measurements of the source signal in Lebinthini species producing harmonic-dominant calling songs have shown that the frequency of their source signal match the value of the non-dominant, low--frequency fundamental [23]. Those measurements, along with our own results using both LDV and modelling with the finite element method, suggest that this mechanism takes place, at least partly, during the second step of the sound-generation process.

4.1. Modelling and comparing the vibro-acoustic behaviours

The first of the two species investigated in this study is *Nisitrus malaya*, which song power spectrum is characterised by a low dominant fundamental frequency and several well-amplified (but non-dominant) harmonics [21]. The LDV data obtained from the forewings of three males show a dominant resonant peak between 6.0 and 7.1 kHz, close to the dominant frequency of the calling song. The modes associated with this dominant resonant frequency show that a large part of the forewing's membrane vibrates in phase, with the harp being the main resonant region in males 1 and 2, while both the harp and the mirror seem to participate equally in the resonant response of male 3. FEM studies of *N. malaya* forewing provide results consistent with the LDV measures when the value of the Young's modulus varies between 7 and 13 GPa for both the membrane and the veins (Fig. 3, Fig. S1). These values fall in the range suggested by studies involving direct measurements of comparable insect wings and cuticular structures [27]. Comparing these results with previous measures of the tooth-strike rate of *N. malaya* during stridulation [23], we can see that the tooth-strike rate falls in the same frequency range as that of the dominant resonant frequency of the membrane, which also corresponds to the fundamental frequency of the calling song. It confirms that the sound-producing mechanism of *N. malaya* is very close to that of model cricket species like *Gryllus bimaculatus* De Geer, 1773 or *Teleogryllus oceanicus* (Le Guillou, 1841): the dominant fundamental frequency of the calling song is produced by the amplification of the dominant frequency of the vibratory signal by the resonant forewings.

The second species investigated is *Ponca hebardi*, a Lebinthini species producing calling songs whose dominant frequency correspond to the third harmonic of the fundamental. The measure of the resonant response of the forewings of this species shows a dominant resonant peak at 21.15 kHz. The resonant mode associated with this peak has a complex shape, and the mirror is the main resonant region. Furthermore, the harp and mirror regions show different resonant responses when examined separately, the harp showing resonant peaks that are not found in the mirror response. The forewings of *N. malaya* and *P. hebardi* therefore show very different vibro-acoustic behaviours involving dominant resonant frequencies completely opposed in terms of frequency values, mode shape, and of main resonant region of the forewing. Comparing the results of the FEM studies in both species suggest that different sets of stiffness parameters are needed to recover resonant frequencies with mode shapes resembling those found in the LDV data (Figs. 5–7). In *Ponca hebardi*, resonant frequencies with mode shapes closer to those measured using the LDV were actually recovered only when the value of Young's modulus of the forewing veins (E_v) was set at least 20 times higher than that of the forewing membranes (E_m). However, it is not necessary for this constraint to be as strong when the FEM incorporate the 3D structure of the forewing, compared to the flat FEM. Results close to those observed for a value of E_v 40 times greater than that of E_m in the flat FEM are obtained

in the 3D FEM when the value of E_v is around 20 times higher than that of E_m. This suggests that the 3D structure of the membrane, even roughly modelled using coordinates of a few landmarks, can strongly contribute to the forewing vibro-acoustic behaviour. Three-dimension configurations of the resonant structures could thus have equivalent effects as deep modifications of the stiffness of the venation on the vibro-acoustic behaviour of this species. While these values for stiffness venation are still very high, they fall in the top of the range of values suggested by the literature for tanned, dry cuticle of insect wings [31].

The 3D structure of the forewing membrane in cricket forewings varies in many ways, which could have a significant differential impact on how the membranes resonate and on the different types of stresses they are subjected to during forewing vibration. Comparing *N. malaya* and *P. hebardi*, we observed that the membrane of *N. malaya* is much smoother than that of *P. hebardi*, where many variations in 3D structure are present, including strong membrane folds along some of the veins. We hypothesise that these folds in the forewing membrane may have an additional constraining effect to that of the general 3D structure, analogous to an increase of the value of vein stiffness as predicted by the *P. hebardi* FEM. The absence of these folds in our models may contribute to the fact that the actual Young's modulus values for this species are not as high as they should be in the FEM. Experimental measurements of the Young's modulus of the membrane and veins of *P. hebardi*, as well as studies of the composition and architecture of the forewing cuticle should be carried out in the future to confirm the existence of such a difference in stiffness in actual forewings.

In addition, the difference between the dominant resonant frequencies of the two species is also related to a difference in the damping properties of the forewing membrane. Our results suggest that the forewings of *P. hebardi* appear to be more damped than those of *N. malaya*. Measurements of Rayleigh damping coefficients in both species (see Tables S1 and S2) also show that the mass-proportionnal coefficient α is always found higher in *P. hebardi* than in *N. malaya*. Although these differences are not sufficient to observe a dominant high-resonant frequency in the *P. hebardi* flat FEM, we can see that the resonant response of the *P. hebardi* FEM display well-amplified high resonant frequencies compared to the response of *N. malaya*.

4.2. The constraining role of veins as a cause of harmonic-hopping in the Lebinthini crickets

Several studies have previously shown that veins can play an important role in the physical properties of insect wings, e.g. during flight, in terms of flexural stiffness and fracture toughness [32]. Our results, in agreement with experimental measurements, show different vibro-acoustic behaviours between the forewing FEMs of *N. malaya* and *P. hebardi*, and identify the role of membrane and vein stiffness, partly mediated by forewing 3D structure, as an important factor in distinguishing their resonant properties. The shape of the dominant resonant mode observed with LDV in the resonant response of *N. malaya* is a simple shape characterised by the simultaneous vibration in phase of several regions of the forewing (see Fig. S2), i.e. the harp, the mirror and the anal region. By comparison, the resonant modes measured in the LDV response of *P. hebardi* are more complex, consisting of several antinodes located in more restricted regions of the forewing. Furthermore, while the resonant responses of the harp and the mirror appear completely similar in the case of *N. malaya*, the results of *P. hebardi* show that the two regions contribute differently to the response of the forewings as a whole.

The results of FEM of the forewings of the two species suggest that these differences are due to a greater constraining role of the venation in the case of *P. hebardi*, modelled by high values of Young's modulus relative to those of the membrane. We suggest that the cause of this increase in stiffness properties could be related to two different types of changes. Firstly, as discussed above, changes in the 3D structure of the forewings, as well as the presence of specific relief structures such as membrane folds observed on real specimens, can contribute to the constraint role on the membrane resonant frequencies. In addition, studies have observed a variety of microscopic forewing ultrastructures and folds in different cricket clades, including the Eneopterinae [33]. The potential effects of these surface ultrastructure on forewing resonant properties have been little studied, but it is likely that they could be involved in modifications of the forewing vibration. Secondly, changes in the composition and structure of the venation cuticle, particularly in the relative amounts of resilin and chitin [34], along with variations in the structural organisation of the cuticle's layers themselves [35] could be related to an increase in the stiffness properties of the veins' material. This constraining role of the forewing veins appears to cause the different regions of the forewing to resonate differently and more independently than in the case of *N. malaya*, allowing specific regions (e.g., the mirror region) to match the frequency value of the harmonic components of the stridulation source signal. By estimating the Rayleigh damping coefficients from the LDV data and integrating the 3D structure of the forewing into the FEM, it was possible to match the amplitudes of the resonant peaks in the FEM response spectrum to what was measured experimentally. The dominant high-frequency resonant peak, close to the value of the dominant third harmonic in the calling song, appears to result from the combined effect of the 3D structure and the damping properties of the forewing membrane. Furthermore, our results show that the value of the damping ratios is not uniform between the different regions of the forewing such as the harp and the mirror (see Table S2). This is another explanation for the difference between the resonant responses of the harp and mirror regions measured on the real forewings of *P. hebardi*. The evolution of the damping properties of the forewing membrane could therefore be one of the mechanisms explaining the phenomenon of harmonic amplification in the sound-production system of the Lebinthini.

4.3. Comparison of harmonic-hopping in Lebinthini and bee hummingbirds

Our results corroborate the hypothesis we investigated in this work, suggesting that harmonic-dominant signals in Lebinthini crickets emerged through acquisition of new resonant properties of the filter over the course of evolutionary history. The description of specific regions of the forewings of *P. hebardi* as "semi-independent" resonant regions with distinct vibro-acoustic behaviour makes it interesting to compare it with another harmonic-hopping mechanism studied in hummingbirds of the genus *Selasphorus* (Mellisugini) [3]. In both cases, the sound-production mechanisms, although very different, can be modelled as source-filter systems. The non-vocal

sounds of bee hummingbirds are produced by the vibration of the birds' tail feathers during diving displays [36]. They are classically characterised by a dominant fundamental frequency produced by one or more feathers, the “source feathers”. The adjacent feathers to which the source feathers are aerodynamically coupled constitute the “filter feathers”. By studying the sounds emitted by several species of bee hummingbirds, Clark and his collaborators showed that significant frequency “jumps” can occur through the gain and loss of source feathers [3]. Clark identified one of these source switches as responsible for a harmonic-hopping phenomenon in the species *Selasphorus sasin* (R. Lesson, 1829), in which the gain of a new source feather shifts the dominant frequency to the second harmonic of the ancestral fundamental frequency [3].

The results obtained when studying the mechanisms underlying harmonic-hopping in Lebinthini crickets and bee hummingbirds seem very different. In the hummingbird *S. sasin*, the emergence of a dominant harmonic frequency in non-vocal sounds of this species is associated with a change in the source of the system (gain of a source feather). In contrast, our results on the Lebinthini species *P. hebardi* show that the harmonic-hopping in this species is linked to a modification of the filter (resonant properties of the forewings). However, the source-filter models describing the sound-producing mechanisms in both cases are of different nature. The source-filter model described by Clark for bee hummingbirds is composed of multiple distinct resonant structures (the feathers) that are associated with one function in the model (source feathers vs filter feathers), and these multiple structures are coupled through aerodynamic interactions [37]. On the contrary, the source-filter model described for crickets is constituted of two structures (the forewings) associated with both the source (the stridulation process) and the filter (the membrane of the forewings). Source and filter are structurally coupled in crickets.

Furthermore, different traits between both cases were identified as being responsible for the modifications in the resonant properties of the sound-producing structures. In the case of *S. sasin*, the evolution of the shapes of vibrating feathers is identified as the main cause of the source switch that caused the harmonic-hopping event in this species' history. Our results for *P. hebardi* suggest that the evolution of both the 3D structure and the physical properties of the forewings' material are the main factors in the occurrence of harmonic-hopping in this species. Evolution of forewings’ shape should nevertheless be investigated on a larger scale in the Lebinthini tribe, as it may be one of the causes explaining the diversity in the nature of dominant harmonic frequencies that emerged through harmonic-hopping in this tribe.

4.4. Limitations in LDV and FEM methodology

This study intended to investigate the difference in resonant properties between two different species of Eneopterinae crickets, in order to infer how dominant harmonic frequencies can be produced in the song of species of the Lebinthini tribe. Although our results provide clues as to how the biophysical properties of the forewings provide a substratum for the harmonic amplification mechanism in cricket songs, certain limitations of our methodology can be highlighted. LDV measurements of the forewings for both species were conducted on fixed and separated forewings, with an excitation force constituted of an acoustic pressure. LDV measurements of forewings engaged during stridulation should be performed in the future, as studies have shown that the coupling of the two forewings plays a major role in tuning the resonant frequencies of the system during sound production [17]. The same limitations apply to the FEM results.

In addition, while the study of the resonant properties of the filter constituted by the forewings is essential to understand the characteristics of the crickets’ calling song, it should not be forgotten that the song produced is born from the interaction of these resonant properties with the vibrational signal generated by the stridulation. In particular, Bennet-Clark and Bailey identified the "ticking" produced by the catching and release of the file teeth by the plectrum as one of the sources of the high-frequency components of the song produced by crickets [30]. It therefore can explain how harmonic frequencies are created during the first step of sound production, and how their interaction with high resonant frequencies of the forewing membrane (Fig. 7) allows them to become dominant in the calling song. The resonant behaviour of forewings subjected to an excitation signal similar to that produced by stridulation should also be studied in the future to fully understand the biomechanics of harmonic amplification in cricket calling songs.

4.5. Discrepancies between LDV and FEM response in P. hebardi

Although the modelled resonant frequencies of *P. hebardi* resemble those found in the resonant response of the real forewings, some gaps remain between the modelled and measured vibro-acoustic behaviours. The resonant frequency f_b whose shape is close to that of the dominant resonant peak in LDV is not the dominant peak in the flat FEM response spectrum (Fig. 6) and is several kHz below the corresponding frequency in the LDV results. The specimen used to study *P. hebardi* was a dried-preserved male forewing separated from the rest of the body of the insect. Several studies have demonstrated that post-mortem desiccation in insects and storage treatment in natural history collections can affect some physical properties of the cuticle in a minor way [28]. We however rehydrated the specimen in a humid chamber, a treatment known to restore Young's modulus and vibrational mechanics of cricket wing to that of live specimens, with the notable exception of damping properties [38]. As our results show that damping properties seem to play an important role in the production of high-amplitude harmonics, this could in part explain the discrepancies found between the measured specimen and our FEM.

Some limitations also remain when comparing the results of the 3D FEM with experimental measurements of the actual forewing's response. While resonant frequencies f'_a and f'_b are similar to those observed in the flat FEM and the LDV results, the anal region plays an important role in the resonance of the 3D FEM at frequency f'_a, which is not the case in the vibro-acoustic behaviour measured with LDV. In the same manner, the harp region is the region of maximum velocity amplitude at resonant frequency f'_b, while the mirror is

supposed to play this role according to experimental data.

The response spectrum of the harp in the FEM shows a single dominant resonant peak corresponding to that of the whole forewing, whereas in the LDV measurements several other well amplified resonant peaks can be observed at lower frequencies (Fig. 7B). The mirror, on the other hand, shows a dominant resonant peak of low frequency value that differs from the response of the whole forewing. This is different from the response of the mirror region measured with LDV, where the dominant resonant peak matches that observed in the response of the whole forewing (Fig. 7C). Furthermore, our results show that, while both the harp and mirror resonances contribute to the dominant resonant peak observed in the whole forewing response, the harp region is clearly the main resonant region of the system. Although this is consistent with what is typically found in other cricket species [16,18], it is not consistent with LDV measures where the mirror is the region that contributes most to the dominant resonant peak in the response spectrum. As the LDV data for the forewing of *P. hebardi* were obtained for a single dry specimen, we are unable to assess the variability that may exist in the resonant responses of several individuals, as to the respective contribution of the harp and mirror regions to the vibro-acoustic behaviour of the forewing as a whole. Forewing measurements from other male specimens of this species should be carried out in the future to address this limitation of our results.

5. Conclusion

This study demonstrates that harmonic-dominant signals in Lebinthini crickets arise from changes in the resonance properties of the forewings. Finite element modelling and laser Doppler vibrometry results reveal that increased vein stiffness, 3D membrane structure, and damping properties all contribute to enable specific forewing regions (the mirror in the case of *P. hebardi*) to amplify harmonic frequencies. These findings shed new light on the biophysical mechanisms underlying harmonic-hopping in Eneopterinae crickets.

CRediT authorship contribution statement

Teddy Gaiddon: Writing – original draft, Visualization, Methodology, Investigation, Formal analysis, Conceptualization. **Thorin Jonsson:** Writing – review & editing, Visualization, Methodology, Investigation, Formal analysis. **Alberto Mittone:** Writing – review & editing, Resources. **Alberto Bravin:** Writing – review & editing, Resources. **Fernando Montealegre-Z:** Writing – review & editing, Resources, Investigation. **Vincent Tournat:** Writing – review & editing, Methodology, Funding acquisition, Conceptualization. **Tony Robillard:** Writing – original draft, Supervision, Resources, Funding acquisition, Conceptualization.

Ethical approval statement

Used specimens were from insect colonies of the Muséum national d'Histoire naturelle (MNHN) of Paris. We declare compliance with the MNHN ethical standards.

Data availability statement

All data will be made available on request. For requesting data, please write to the corresponding author.

Funding

This work was conducted as part of the doctoral thesis of Teddy Gaiddon, entitled "Harmonic-hopping in the calls of Lebinthini crickets: input from comparative finite element modelling and geometric morphometrics " at the Muséum national d'Histoire naturelle, Paris, France, under the supervision of Tony Robillard and Vincent Tournat. The thesis was funded by Initiative Biodiversité, Évolution, Écologie, Société (IBEES) of the Alliance Sorbonne Université. Fernando Montealegre-Z was funded by the Natural Environment Research Council (NERC), [Grant DEB-1937815]. Thorin Jonsson has received funding from the European Union's Horizon 2020 Research and Innovation Programme under the Marie Skłodowska-Curie grant agreement (no. 829208, InWingSpeak) and from the Austrian Science Fund (FWF; 10.55776/P35792).

Declaration of competing interest

The authors declare that they have no known competing financial interests or personal relationships that could have appeared to influence the work reported in this paper.

Acknowledgments

We thank André Nel and Thomas Schubnel from the Muséum national d'Histoire naturelle (MNHN) of Paris for their help with CT-scan acquisitions and data treatment. We also thank Maxime Grosmougin for his assistance in acquiring 3D landmarks using MicroVu Vertex 251 and Inspec software. Preliminary data from this research were presented at the 3rd African Bioacoustics Community Conference (ABC) 2022 in Kruger National Park, South Afrika, and at the Invertebrate Sound and Vibration (ISV) 2023, Lincoln, United Kingdom.

Appendix A. Supplementary data

Supplementary data to this article can be found online at https://doi.org/10.1016/j.heliyon.2025.e44424.

References

[1] J.W. Bradbury, S.L. Vehrencamp, Principles of Animal Communication, second ed., Sinauer Associates, 2011.
[2] R.D. Patterson, Pulse-resonance sounds, in: D. Jaeger, R. Jung (Eds.), Encyclopedia of Computational Neuroscience, Springer, New York, NY, 2014, pp. 1–8, https://doi.org/10.1007/978-1-4614-7320-6_430-6.
[3] C.J. Clark, Harmonic hopping, and both punctuated and gradual evolution of acoustic characters in selasphorus hummingbird tail-feathers, PLoS One 9 (2014) e93829, https://doi.org/10.1371/journal.pone.0093829.
[4] N.H. Fletcher, Acoustic Systems in Biology, Oxford University Press, 1992.
[5] C. Niezrecki, R. Phillips, M. Meyer, D.O. Beusse, Acoustic detection of manatee vocalizations, J. Acoust. Soc. Am. 114 (2003) 1640–1647, https://doi.org/10.1121/1.1598196.
[6] J.K.B. Ford, B. Koot, S. Vagle, N. Hall-Patch, G. Kamitakahara, Passive Acoustic Monitoring of Large Whales in Offshore Waters of British Columbia, vol. 2898, Canadian Technical Report of Fisheries and Aquatic Sciences, 2010. https://publications.gc.ca/pub?id=9.619999&sl=1.
[7] T. Kingston, S.J. Rossiter, Harmonic-hopping in Wallacea's bats, Nature 429 (2004) 654–657, https://doi.org/10.1038/nature02487.
[8] C.J. Clark, J.A. McGuire, E. Bonaccorso, J.S. Berv, R.O. Prum, Complex coevolution of wing, tail, and vocal sounds of courting male bee hummingbirds, Evolution 72 (2018) 630–646, https://doi.org/10.1111/evo.13432.
[9] R. Marquez, I. Riva, J. Bosch, Advertisement calls of Bolivian Leptodactylidae (Amphibia, Anura), J. Zool. 237 (1995) 313–336, https://doi.org/10.1111/j.1469-7998.1995.tb02765.x.
[10] F. Montealegre-Z, G.K. Morris, Songs and systematics of some Tettigoniidae from Colombia and Ecuador I, Pseudophyllinae (Orthoptera), J. Orthoptera Res. 8 (1999) 163–236, https://doi.org/10.2307/3503439.
[11] T. Robillard, P. Grandcolas, L. Desutter-Grandcolas, A shift toward harmonics for high-frequency calling shown with phylogenetic study of frequency spectra in Eneopterinae crickets (Orthoptera, Grylloidea, Eneopteridae), Can. J. Zool. 85 (2007) 1264–1275, https://doi.org/10.1139/Z07-106.
[12] M.M. Cigliano, H. Braun, D.C. Eades, D. Otte, Orthoptera species file, in: O. Bánki, Y. Roskov, M. Döring, G. Ower, D.R. Hernández Robles, C.A. Plata Corredor, T. Stjernegaard Jeppesen, A. Örn, L. Vandepitte, D. Hobern, P. Schalk, R.E. DeWalt, K. Ma, J. Miller, T. Orrell, R. Aalbu, J. Abbott, R. Adlard, C. Aedo, et al., Catalogue of Life Checklist (2025), Species File Group. http://orthoptera.speciesfile.org/otus/831487/overview (accessed December 12, 2025).
[13] M.K. Tan, J. Malem, F. Legendre, J. Dong, J.B. Baroga-Barbecho, S.A. Yap, et al., Phylogeny, systematics and evolution of calling songs of the Lebinthini crickets (Orthoptera, Grylloidea, Eneopterinae), with description of two new genera, Syst. Entomol. 46 (2021) 1060–1087, https://doi.org/10.1111/syen.12510.
[14] H.C. Bennet-Clark, Songs and the physics of sound production, in: F. Huber, T.E. Moore, W. Loher (Eds.), Cricket Behavior and Neurobiology, Cornell University Press, 1989, pp. 227–261, https://doi.org/10.7591/9781501745904.
[15] H.M. ter Hofstede, S. Schöneich, T. Robillard, B. Hedwig, Evolution of a communication system by sensory exploitation of startle behavior, Curr. Biol. 25 (2015) 3245–3252, https://doi.org/10.1016/j.cub.2015.10.064.
[16] H.C. Bennet-Clark, Resonators in insect sound production: how insects produce loud pure-tone songs, J. Exp. Biol. 202 (1999) 3347–3357, https://doi.org/10.1242/jeb.202.23.3347.
[17] T. Jonsson, F. Montealegre-Z, C.D. Soulsbury, D. Robert, Tenors not sopranos: bio-mechanical constraints on calling song frequencies in the Mediterranean field-cricket, Front. Ecol. Evol. 9 (2021) 647786, https://doi.org/10.3389/fevo.2021.647786.
[18] H. Nocke, Biophysik der Schallerzeugung durch die Vorderflügel der Grillen, Z. Für Vgl, Physiologist 74 (1971) 272–314, https://doi.org/10.1007/BF00297730.
[19] H.C. Bennet-Clark, Wing resonances in the Australian field cricket Teleogryllus oceanicus, J. Exp. Biol. 206 (2003) 1479–1496, https://doi.org/10.1242/jeb.00281.
[20] T. Robillard, H.M. ter Hofstede, J. Orivel, N.M. Vicente, Bioacoustics of the neotropical eneopterinae (Orthoptera, grylloidea, Gryllidae), Bioacoustics 24 (2015) 123–143, https://doi.org/10.1080/09524622.2014.996915.
[21] M.K. Tan, H.A. Wahab R bin, R. Japir, A.Y.C. Chung, T. Robillard, Revision of the cricket genus Nisitrus Saussure (Orthoptera: gryllidae: eneopterinae) and descriptions of five new species, Eur. J. Taxon. 761 (2021) 1–75, https://doi.org/10.5852/ejt.2021.761.1449.
[22] J.L. Benavides-Lopez, H. ter Hofstede, T. Robillard, Novel system of communication in crickets originated at the same time as bat echolocation and includes Male-Male multimodal communication, Sci. Nat. 107 (2020) 9, https://doi.org/10.1007/s00114-020-1666-1.
[23] T. Robillard, F. Montealegre-Z, L. Desutter-Grandcolas, P. Grandcolas, D. Robert, Mechanisms of high frequency song generation in brachypterous crickets and the role of ghost frequencies, J. Exp. Biol. 216 (2013) 2001–2011, https://doi.org/10.1242/jeb.083964.
[24] F. Montealegre-Z, T. Jonsson, D. Robert, Sound radiation and wing mechanics in stridulating field crickets (Orthoptera: gryllidae), J. Exp. Biol. 214 (2011) 2105–2117, https://doi.org/10.1242/jeb.056283.
[25] A. Mittone, I. Manakov, L. Broche, C. Jarnias, P. Coan, A. Bravin, Characterization of a sCMOS-based high-resolution imaging system, J. Synchrotron Radiat. 24 (2017) 1226–1236, https://doi.org/10.1107/S160057751701222X.
[26] A. Mirone, E. Brun, E. Gouillart, P. Tafforeau, J. Kieffer, The PyHST2 hybrid distributed code for high speed tomographic reconstruction with iterative reconstruction and a priori knowledge capabilities, Nucl. Instrum. Methods Phys. Res. Sect. B Beam Interact. Mater. Atoms 324 (2014) 41–48, https://doi.org/10.1016/j.nimb.2013.09.030.
[27] J.F.V. Vincent, U.G.K. Wegst, Design and mechanical properties of insect cuticle, Arthropod Struct. Dev. 33 (2004) 187–199, https://doi.org/10.1016/j.asd.2004.05.006.
[28] D. Klocke, H. Schmitz, Water as a major modulator of the mechanical properties of insect cuticle, Acta. Biomaterials 7 (2011) 2935–2942, https://doi.org/10.1016/j.actbio.2011.04.004.
[29] N. Mhatre, F. Montealegre-Z, R. Balakrishnan, D. Robert, Changing resonator geometry to boost sound power decouples size and song frequency in a small insect, Proc. Natl. Acad. Sci. USA 109 (2012) E1444–E1452, https://doi.org/10.1073/pnas.1200192109.
[30] H.C. Bennet-Clark, W.J. Bailey, Ticking of the clockwork cricket: the role of the escapement mechanism, J. Exp. Biol. 205 (2002) 613–625, https://doi.org/10.1242/jeb.205.5.613.
[31] J.H. Dirks, D. Taylor, Fracture toughness of locust cuticle, J. Exp. Biol. 215 (2012) 1502–1508, https://doi.org/10.1242/jeb.068221.
[32] J.H. Dirks, D. Taylor, Veins improve fracture toughness of insect wings, PLoS One 7 (2012) e43411, https://doi.org/10.1371/journal.pone.0043411.
[33] L. Desutter-Grandcolas, Functional forewing morphology and stridulation in crickets (Orthoptera, Grylloidea), J. Zool. 236 (1995) 243–252, https://doi.org/10.1111/j.1469-7998.1995.tb04491.x.
[34] J. Michels, E. Appel, S.N. Gorb, Functional diversity of resilin in arthropoda, Beilstein J. Nanotechnol. 7 (2016) 1241–1259, https://doi.org/10.3762/bjnano.7.115.
[35] C.S. Sample, A.K. Xu, S.M. Swartz, L.J. Gibson, Nanomechanical properties of wing membrane layers in the house cricket (Acheta domesticus Linnaeus), J. Insect Physiol. 74 (2015) 10–15, https://doi.org/10.1016/j.jinsphys.2015.01.013.

[36] C.J. Clark, T.J. Feo, I. Escalante, Courtship displays and natural history of scintillant (Selasphorus scintilla) and Volcano (S. flammula) hummingbirds, Wilson J. Ornithol. 123 (2011) 218–228, https://doi.org/10.1676/10-076.1.
[37] C.J. Clark, D.O. Elias, R.O. Prum, Aeroelastic flutter produces hummingbird feather songs, Science 333 (2011) 1430–1433, https://doi.org/10.1126/science.1205222.
[38] R. Weiner, S. Duke, G. Simonelli, N.W. Bailey, N. Mhatre, Reliable reconstruction of cricket song from biophysical models and preserved specimens, R. Soc. Open Sci. 12 (2025) 251005, https://doi.org/10.1098/rsos.251005.